Polarimetric Signature Imaging of Anisotropic Bio-Medical Tissues

Stewart H. Wu[1], Soe-Mie F. Nee[2], De-Ming Yang[3, 4], Arthur Chiou[4] and Tsu-Wei Nee*[2]

[1] Taiwan Semiconductor Manufacturing Company, Ltd., Hsinchu 30844, Taiwan
[2] Neopola Optical Analysis, Inc., Richmond, CA 94804, U. S. A.
[3] Taipei Veterans General Hospital, Taipei 11217, Taiwan
[4] Institute of Biophotonics, National Yang Ming University, Taipei 11221, Taiwan
*Corresponding author: tsuw.nee@gmail.com

***Abstract*- Polarimetric imaging of Stokes vector (*I, Q, U, V*) can provide independent signatures of polarization and depolarization of biological tissues and cells. Using a Stokes digital imaging system, we measured the Stokes vector images of tissue samples from sections of rat livers. The derived Mueller matrix elements can quantitatively provide five-signature (m_{01}, m_{11}, m_{22}, m_{23} and m_{33}) imaging data for the bio-sample. The images of four independent optical properties: linear-dichroic polarization, depolarization, cross-polarized depolarization and phase retardation of the test sample are then derived. The probability distribution for these parameters can also be obtained from the imaging data. Based upon the anisotropic orientation distribution of ellipsoid model bio-molecules, five matrix elements, m_{01}, m_{11}, m_{22}, m_{23} and m_{33} were simulated to obtain the estimated optical properties to compare with those measured properties of the sample. This polarimetric multi-signature optical technology is a new option of biosensing technology to inspect the structures of tissue samples and is useful for critical disease discrimination and medical diagnostics applications.**

Keywords– Polarimetric Mueller Matrix Imaging; Bio-Medical Tissues; Anisotropic and Photon-Scattering Signatures

I. INTRODUCTION

Molecular imaging technology of bio-medical materials such as cell, protein, tissue, etc. is of major interest in biophotonics [1]. Bio-medical materials are, in general, optically anisotropic and highly photon-scattering [2]. The anisotropic property of bio-medium can be determined from the polarization properties of light scattered and/or transmitted from the medium. Polarization is a basic property of light. Fluorescence polarization has been developed for bio-technology applications [3, 4]. The single-molecule fluorescence polarization imaging of anisotropic TMR-labeled lipid molecule in a 1-palmitoyl-2-oleoyl-sn-glycerol-3-phosphocholine (POPC) membrane and eYFP (enhanced yellow-fluorescent protein) has been demonstrated [5, 6]. The linear and non-linear full polarization optical properties of an anisotropic object, material or device, can be completely described by a 4 × 4 Mueller matrix [7, 8, 9, 10]. The Mueller matrix modeling theory has recently been developed for investigating the optical polarization property of bio-molecule and highly scattering membrane bio-medium. The fitting between the theory and the anisotropic imaging data of ref. 6 has been shown to be satisfactory [11, 12]. The Mueller matrix imaging systems have been recently developed for investigating the optical polarization property of bio-medical tissues [13 - 16]. Similar to other polarimetric investigations [5, 17 - 19], the optical systems and the imaging data results were reported.

There exist very few physical models for the understanding of the fundamental optical polarization properties of bio-samples. Our theory has provided a foundation for the simulation analysis of the polarization properties of bio-molecular media, and has correlated the polarization optical signatures of a bio-molecule with its microscopic electronic structure [11, 12]. Based on double photon scattering, the degrees of linear-dichroic polarization scattering by a bio-molecular medium was numerically calculated [12] and fitted to an experiment [5]. The Mueller matrix results have shown that the bio-medium is optically anisotropic ($m_{01} \neq 0$) and highly scattering but not perfectly diffusive ($m_{11} = 0.3454 < 1$ in eq.19 of ref. 12). Therefore, the Mueller Stokes imaging technology based upon the five principal Mueller matrix elements m_{01}, m_{11}, m_{22}, m_{23} and m_{33} is feasible for investigating the anisotropic, photon-scattering and polarization/depolarization optical properties of bio-medical medium.

To explore the potential biomedical application and to understand the anisotropic optical property of biological samples, we have developed a simple experiment for Stokes vector imaging measurement. We chose a forward transmission optical design in a microscope system which is described in the next section. Three experimental steps were used to get the Mueller matrix signature of the bio-sample under investigation. The measured images of four independent polarization parameters and the derived distribution functions of five principal Mueller matrix elements are reported in section III. A biomedical discrimination application example is also shown in section III. The discussion and conclusions are given in the final section.

II. MUELLER STOKES IMAGING METHOD

A. Experimental Setup

A schematic diagram of our setup is shown in Fig. 1. A 150 W halogen lamp is connected to an optical fiber pipe to

provide the white light source. After the light source and a 570 – 610 nm band-pass filter, a Glan-Thompson polarizer was used to provide a linearly polarized light incident on the sample where the polarization direction could be varied by rotating the polarizer. An optional linear polarizer (a second Glan-Thompson polarizer) and/or quarter wave plate were used in the analyzer part to analyze the Stokes vector (I, Q, U, V) of light exiting the sample. The 600 × 800 CCD imager has a FOV (field of view) of 144 × 192 (μm^2). Each pixel corresponds to an area ~ 240 × 240 nm^2 at the sample plane.

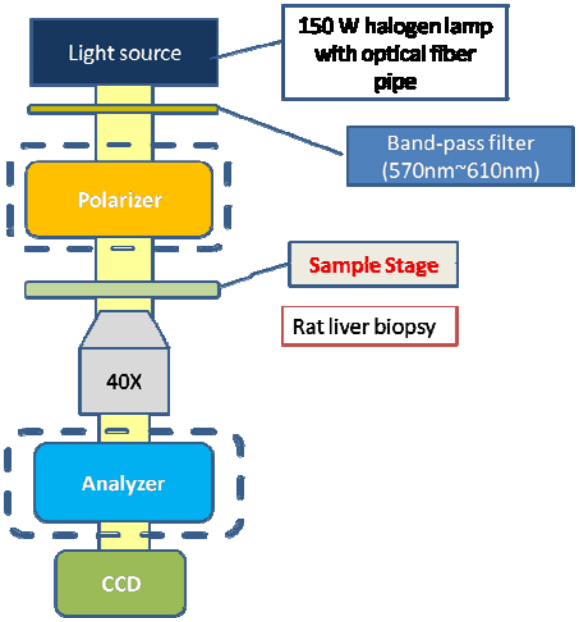

Fig. 1 A schematic diagram of the experiment setup

B. Stokes Vector Measurement

The Stokes vector $\mathbf{S} = (I, Q, U, V)$ of light is

$$\mathbf{S} = \begin{pmatrix} I \\ Q \\ U \\ V \end{pmatrix} = I \begin{pmatrix} 1 \\ q \\ u \\ v \end{pmatrix} = \begin{pmatrix} I_0 + I_{90} \\ I_0 - I_{90} \\ I_{45} - I_{-45} \\ I_r - I_l \end{pmatrix}. \quad (1)$$

To measure I, Q, U, only a linear polarizer is used in the analyzer part. Four measurements are performed in the sequence of 0, 90°, 45° and – 45°. The images of I, q, u are obtained from the measured I_0, I_{90}, I_{45} and I_{-45}.

For incident light with Stokes vector $\mathbf{S}_i = I_i\,(1, q_i, u_i, v_i)$, the Stokes vector of transmitted light is $\mathbf{S}_t = I_i\,(1, q_t, u_t, v_t) = \mathbf{M}\,\mathbf{S}_i$. The following are the three steps taken in the experiment:

Step A: $\mathbf{S}_1 = I_1\,(1, q_1, u_1, v_1) = \mathbf{M}\,S_{i1}$. Parameters q_1 and u_1 were measured. $\mathbf{S}_{i1} = \mathbf{M}_1\,\mathbf{S}_i$ is the incident Stokes vector for $\mathbf{M}_1$, which corresponds to the Mueller matrix with the linear polarizer set at 0°.

Step B: $\mathbf{S}_2 = I_2\,(1, q_2, u_2, v_2) = \mathbf{M}\,S_{i2}$. Parameters q_2 and u_2 were measured. $\mathbf{S}_{i2} = \mathbf{M}_2\,\mathbf{S}_i$ is the incident Stokes vector for $\mathbf{M}_2$, which corresponds to the Mueller matrix with the linear polarizer set at 90°.

Step C: $\mathbf{S}_3 = I_3\,(1, q_3, u_3, v_3) = \mathbf{M}\,S_{i3}$. Parameters q_3 and u_3 were measured. $\mathbf{S}_{i3} = \mathbf{M}_3\,\mathbf{S}_i$ is the incident Stokes vector for $\mathbf{M}_3$, which corresponds to the Mueller matrix with the right-hand circularly polarizer set.

C. Mueller Matrix Determination

We consider that the investigated samples are not optically active so that circular dichroism and circular birefringence are negligible. Assume that incident light is normal to the sample surface. The laboratory coordinates (x, y, z) are chosen such that the direction of incident light is $\hat{k}_i = (0, 0, 1)$ and the sample surface is the xy-plane. Let the directions of the principal axes of the sample be $\hat{e}_1 = (\cos\theta, \sin\theta, 0)$ and $\hat{e}_2 = (-\sin\theta, \cos\theta, 0)$. Then the Mueller matrix for the normal transmission of the sample is [7, 20]

$$\mathbf{M} = \mathbf{R}^{-1}(\theta)\,\mathbf{M}_o\,\mathbf{R}(\theta); \quad (2)$$

$$\mathbf{M}_o = T\begin{pmatrix} 1 & m_{01} & 0 & 0 \\ m_{01} & m_{11} & 0 & 0 \\ 0 & 0 & m_{22} & m_{23} \\ 0 & 0 & -m_{23} & m_{33} \end{pmatrix}, \tag{3a}$$

$$\mathbf{R}(\theta) = \begin{pmatrix} 1 & 0 & 0 & 0 \\ 0 & \cos 2\theta & \sin 2\theta & 0 \\ 0 & -\sin 2\theta & \cos 2\theta & 0 \\ 0 & 0 & 0 & 1 \end{pmatrix}; \tag{3b}$$

$$\begin{aligned} m_{11} &= 1 - 2\mathcal{D}_v, \\ \mathcal{P}^2 &= m_{01}^2 + m_{23}^2 + (m_{22}^2 + m_{33}^2)/2, \\ \mathcal{D} &= 1 - \mathcal{P} = \mathcal{D}_u + \mathcal{D}_v. \end{aligned} \tag{4}$$

Here $\mathbf{M}_o$ is the sample Mueller matrix in the principal frame, and $\mathbf{M}$ is in the laboratory frame. $\mathbf{R}(\theta)$ is the rotation matrix that transforms a Stokes vector in the laboratory frame to the principal frame. In different chosen coordinate systems, θ are different so that $\mathbf{M}$ are also different. For nonzero θ, most m_{ij} are not zero except m_{03} and m_{30} since we consider the sample not optically active. T is the transmittance of the sample. Element m_{01} is the result of linear dichroism and represents the linear-dichroic polarization. Element m_{11} relates directly to the cross-polarized depolarization $\mathcal{D}_v$. Element m_{23} is majorly caused by linear birefringence and represent the linear-birefringent polarization. $\mathcal{P}$, $\mathcal{D}$, and $\mathcal{D}_u$ are the polarization, depolarization, and co-polarized depolarization respectively. The ellipsometric parameters ψ and Δ can then be determined by [7].

$$\begin{aligned} m_{01} &= -\mathcal{P}\cos 2\psi, \\ m_{23} &= \mathcal{P}\sin 2\psi \sin \Delta. \end{aligned} \tag{5}$$

With simple mathematical algorithm, the six parameters m_{01}, m_{11}, m_{22}, m_{23}, m_{33} and θ can be determined from the six measured data of q_1, u_1, q_2, u_2, q_3 and u_3 [20]. The results are

$$\tan 2\theta = [u_1 + u_2 + u_1q_2 - u_2q_1]/(q_1 + q_2), \tag{6a}$$

$$m_{01} = \frac{q_1 + q_2}{(2 + q_2 - q_1)\cos 2\theta}, \tag{6b}$$

$$m_{11} = (X_a + X_b \tan 2\theta)/2, \tag{6c}$$

$$m_{22} = \frac{X_a}{2} - \frac{q_1 + q_2}{2 + q_2 - q_1}, \tag{6d}$$

$$m_{23} = \frac{m_{01}\sin 2\theta - u_3}{\cos 2\theta}, \tag{6e}$$

$$m_{33} = -q_3. \tag{6f}$$

where

$$\begin{aligned} X_a &= q_1 - q_2 + \frac{(q_1 + q_2)^2}{2 + q_2 - q_1}, \\ X_b &= u_1 - u_2 + (u_1 + u_2)\frac{q_1 + q_2}{2 + q_2 - q_1}. \end{aligned} \tag{7}$$

For diploe scattering by random ellipsoids, m_{01} is negative [21]. For simplicity and convenience, we use the positive $|m_{01}|$ values for presentation.

III. POLARIZATION IMAGES AND DISTRIBUTIONS

A. Measurement Tests

For a given image pixel (i, j), the data of $|m_{01}(i, j)|$, $m_{11}(i, j)$, $m_{22}(i, j)$, $m_{23}(i, j)$ and $m_{33}(i, j)$ were calculated using Eqs. (6a) - (7). The probability distributions $f(\xi)$ ($\xi = |m_{01}|$, m_{11}, m_{22}, m_{23}, m_{33}, $0 < \xi < 1$) can be obtained by the histogram function of a graphing software. In this work, we wrote a computer program to count the occurrence of the data in 1000 equal interval ranges $\Delta\xi$ at ξ_j ($\Delta\xi = 0.001$, $\xi_j = j\Delta\xi$) and then normalized it such that the total area under $f(\xi)$ is equal to 1. The five signatures

m_{01}, m_{11}, m_{22}, m_{23}, m_{33} for the transmission through a glass plate sample were measured. Theoretically the expected Mueller matrix is a 4 × 4 unit matrix. The Mueller matrix elements m_{01}, m_{11}, m_{22}, m_{23}, m_{33} should be equal to 0, 1, 1, 0, 1 respectively. As shown in Fig. 2, the measured ξ peak values were equal to 0.03, 0.95, 0.95, 0.06 and 0.93 respectively. These data confirm that the experiment setup was working. The additional little peak signals are due to the square shape of Glan-Thompson prism. When we rotated the prisms in the polarizer and analyzer paths to acquire images, the incident light could not transmit fully due to the partially overlapped area being about 85% as shown in figure. Some of the images might induce a little error when we calculated and compiled the statistics of the signature distributions.

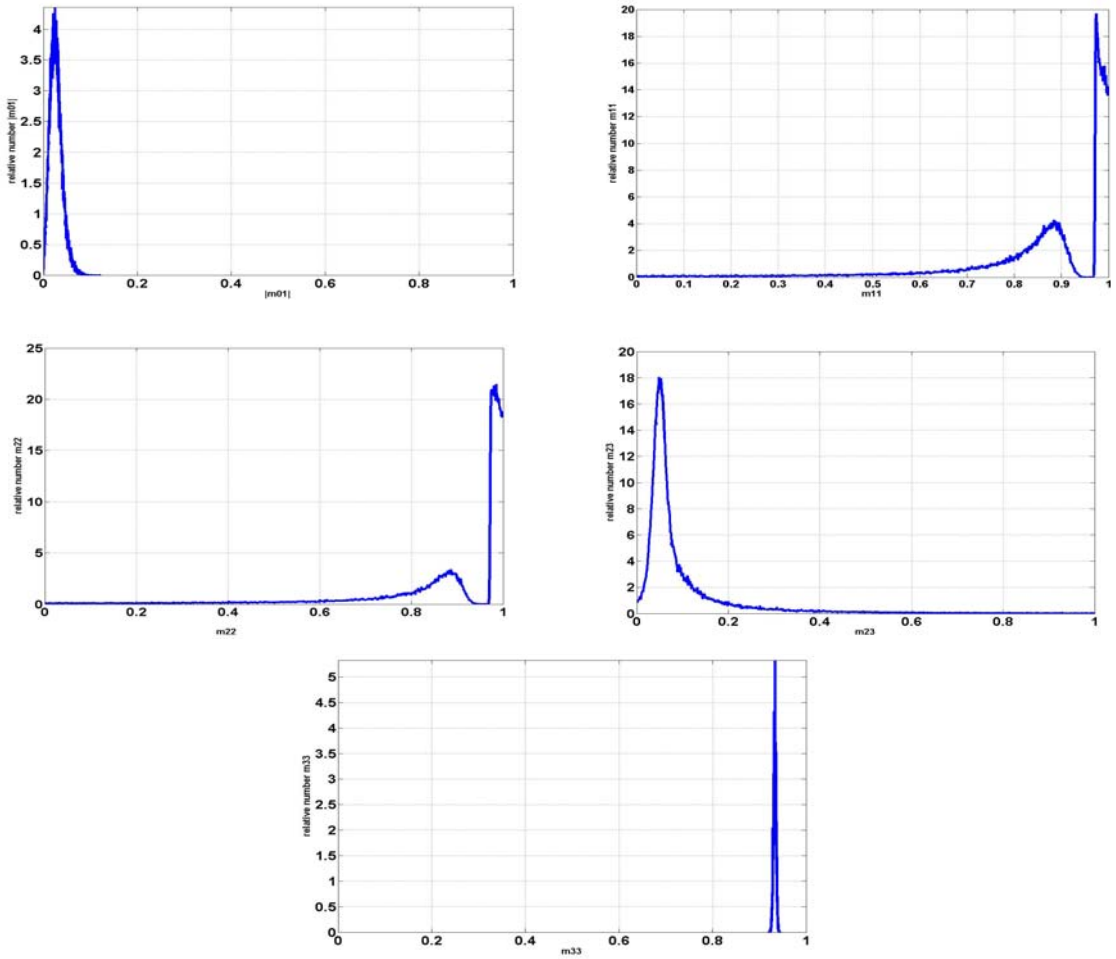

Figure 2 Measured imaging probability distribution functions $f(|m_{01}|)$, $f(m_{11})$, $f(m_{22})$, $f(m_{23})$ and $f(m_{33})$ of a glass plate sample.

Three Liposyn II Intravenous emulsion solution samples were also tested. The solution concentrations were 0.1%, 1% and 10%. These samples were used to simulate the body fat. The measured distribution $f(m_{11})$ for the three concentrations are shown in Fig. 3. The $f(m_{11})$ for the 10% concentration solution peaks near 0, that for the 1% concentration peaks near 0.3, and that for the 0.1% concentration peaks near 1. The three $f(m_{11})$ curves have demonstrated large difference of scattering effect. The photon scattering of 0.1% concentration sample is very small and the 10% sample is nearly diffusive.

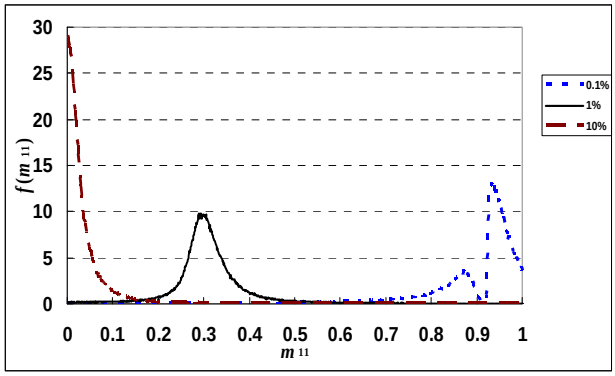

Figure 3 Measured imaging $f(m_{11})$ of three Liposyn II Intravenous emulsion solution samples with concentrations 0.1%, 1 % and 10%.

B. Polarization Images for Bio-Medical Tissue

A sample of non-tumor (NT) rat liver tissue of 3 μm thickness was measured. Figure 4 is the image of $|m_{01}|$ that shows the spatial distribution of linear-dichroic polarization. The scale is set such that black is for $|m_{01}| = 0$ and white is for $|m_{01}| = 1$. The effect of m_{01} is to transform between unpolarised light and linearly polarized light. For example, a good polarizer has a large $|m_{01}|$. Similarly, the image of m_{11} for the sample is shown in Fig. 5. The scale is black for $m_{11} = 0$ (diffusion limit) and white for $m_{11} = 1$ (no scattering). Reduction of m_{11} from 1 is caused by the cross-polarized depolarization of photon scattering. Obviously, the spatial distributions of m_{01} and m_{11} are very different.

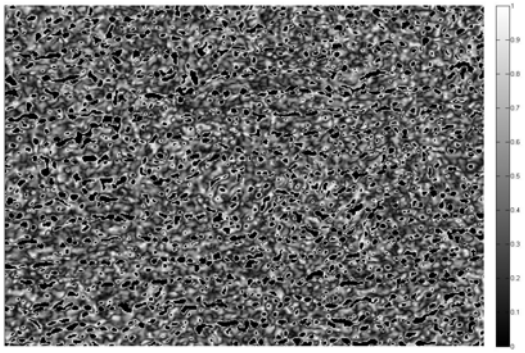

Fig. 4 The image of $|m_{01}|$ for a non-tumor rat liver tissue. The marked scale is black for $|m_{01}| = 0$ and white for $|m_{01}| = 1$.

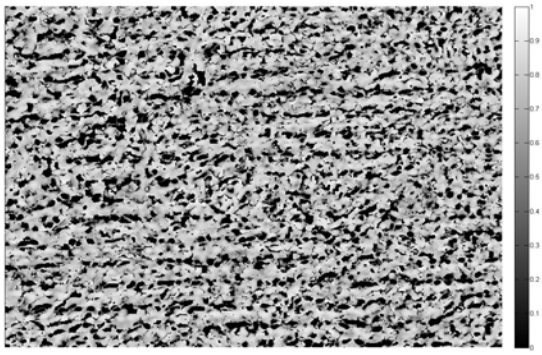

Figure 5 The image of m_{11} for a non-tumor rat liver tissue. The scale is black for $m_{11} = 0$ and white for $m_{11} = 1$

Using the data of $|m_{01}(i, j)|$, $m_{11}(i, j)$, $m_{22}(i, j)$, $m_{23}(i, j)$ and $m_{33}(i, j)$ for each image pixel, the pixel's depolarization $\mathcal{D}(i, j)$, and ellipsometric parameters $\psi(i, j)$ and $\Delta(i, j)$ are calculated using Eq.s (4) and (5). The image of depolarization $\mathcal{D}$ is shown in Figure 6. The scale is black for $\mathcal{D} = 0$ (no depolarization) and white for $\mathcal{D} = 1$ (diffusion limit). The depolarization here is a result of photon scattering. Apparently, m_{11} of Fig. 5 and $\mathcal{D}$ of Fig. 6 are sort of complementary. The image of the phase retardation Δ is shown in Fig. 7, the scale is black for $\Delta = 0^o$ and white for $\Delta = 90°$. This picture is kind of dark indicating that the sample birefringence is very small. The polarization images and distribution of m_{01}, m_{11}, $\mathcal{D}$ and Δ of a bio-tissue are four independent optical signatures that can be useful as clinical diagnostic tool for medical application.

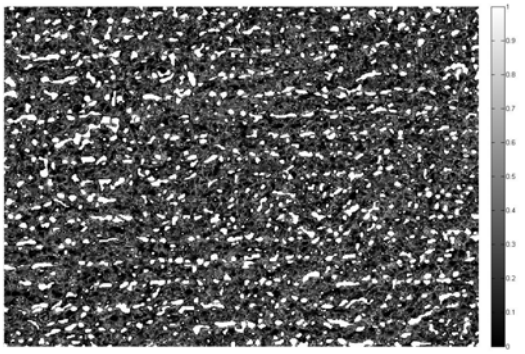

Fig. 6The image of depolarization $\mathcal{D}$ for a non-tumor rat liver tissue. The marked scale is black for $\mathcal{D} = 0$ and white for $\mathcal{D} = 1$.

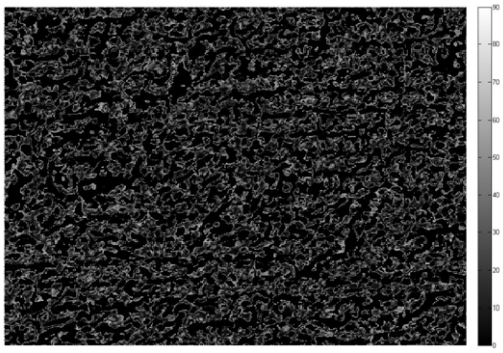

Fig. 7 The image of phase retardation Δ for a non-tumor rat liver tissue. The scale is black for $\Delta = 0^o$ and white for $\Delta = 90^o$.

C. Polarization Distributions for bio-medical tissue

The probability distribution functions $f(|m_{01}|)$, $f(m_{11})$, $f(m_{22})$, $f(m_{23})$ and $f(m_{33})$ are obtained from the corresponding images of m_{ij} and are shown in Fig. 8. $f(|m_{01}|)$ has a peak near 0.3 with a broad width of about 0.42. It means that the tissue elements imaged by each pixel show certain degrees of linear dichroism and most of them contribute to m_{01} near 0.3. $f(m_{11})$ has a peak near 0.81 with a width of about 0.14. If the sample has negligible depolarization, then m_{11} should be close to 1 as manifested by Fig. 2b. Apparently the sample gives considerable depolarization as light passes through it. $f(m_{22})$ has a peak near near 0.79 with a width of about 0.22. The peak position of $f(m_{22})$ is slightly smaller than the peak position of $f(m_{11})$. It means that the sample has very small linear birefringence. $f(m_{33})$ has a peak near near 0.76 with a width of about 0.44. In both $f(m_{22})$ and $f(m_{33})$, the scattering shifts more of these m_{22} and m_{33} toward the smaller values than larger values from the peaks. The width of $f(m_{33})$ is much wider than the width of $f(m_{22})$, this indicates again that the sample gives considerable depolarization as light passes through it. In the figure for $f(m_{23})$, we did not plot those for negative m_{23} since $f(-m_{23})$ is about the same as $f(m_{23})$. Most of m_{23} are near zero such that their average is about zero.

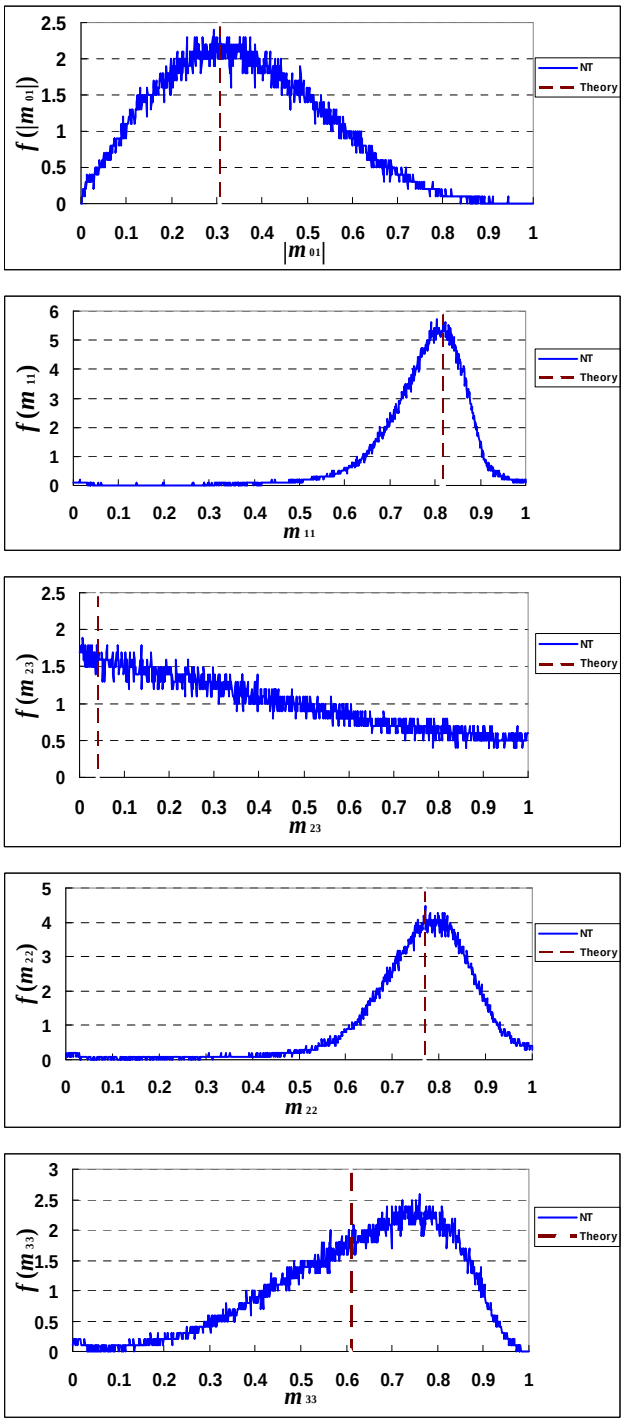

Fig. 8 The measured imaging $f(|m_{01}|)$, $f(m_{11})$, $f(m_{23})$, $f(m_{22})$ and $f(m_{33})$ of a non-tumor rat liver tissue. Theoretical fitting data are marked as vertical lines.

D. Theoretical Fittings

We had fitted these data using our double scattering model [12, 20] with the following parameters:

(1) A model distribution function of dipole orientation is assumed as shown in Figure 9. For mathematical simplicity, the angle θ_d between the molecules' symmetric z_d-axis and the laboratory z-axis is within a specific range (0, θ_{do}). The maximum molecular orientation distribution angle for fitting is chosen as $\theta_{do} = 168^o$.

(2) The model molecule is a uniaxially symmetric ellipsoid with material complex dielectric constant ε_o = (2.06, 0.01). This ε_o was chosen to give the average index of refraction $\langle n \rangle \approx 1.4$ and the average absorption extinction coefficient $\langle \kappa_a \rangle \approx 0.003$ that are the typical measured values for tissues [2, 22 - 24]. The average is performed over the distribution of dipole orientation of Fig. 9.

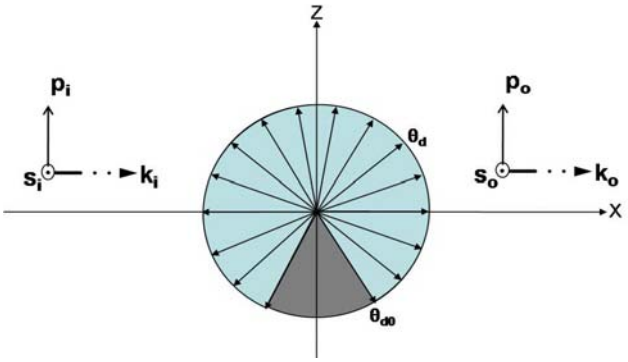

Figure 9 Molecular orientation distribution model and the propagating directions and polarizations of incident and transmitted p-waves.

(3) $b/a = 6$. b and a are the ellipsoid principal radii along the symmetric and the transverse axes respectively [11, 12]. $b/a = 6$ might be a reasonable average value for the long molecules in most tissues.

(4) $d/\lambda = 6$. d is the sample thickness (≈ 3.0 μm), and λ is the photon wavelength (≈ 0.5 μm).

(5) The double scattering strength parameter $\eta_a = 0.4$. As defined in Ref. 12, $\eta_a = r_a/r_o$, $r_a = 4\pi^2a^3/3\lambda^2$, r_o is the inter-scattering distance parameter and is a decreasing function of the molecular density. Therefore, η_a is an increasing function of the molecular density of the medium. $\eta_a = 0$ for single scattering only, and $\eta_a > 0$ for non-vanishing double scattering.

(6) The scattering extinction coefficient parameter $r_{ks} = (\pi^2a^4)/(3\lambda^3b) = 0.001$. The anisotropic scattering extinction coefficient is defined as $\kappa_{sj} = r_{ks}\sigma_{sj}/(r_a^2)$. σ_{sj} is the total molecular scattering cross section. The parameters chosen above are summarized in Table I.

TABLE I. CHOSEN PARAMETERS FOR SIMULATION

b/a	6	ε_o	(2.06, 0.01)
d/λ	6	$(\langle n\rangle, \langle\kappa_a\rangle)$	(1.4, 0.003)
λ (μm)	0.5	$(\Delta n, \Delta\kappa_a)$	$(1.6\times10^{-3}, 2.2\times10^{-4})$
η_a	0.4	$\langle\varepsilon\rangle$	(1.96, 0.008)
a/λ	0.122	$\Delta\varepsilon$	$(4.4\times10^{-3}, 7.1\times10^{-5})$
r_a/λ	0.024	$\langle\kappa_s\rangle$	0.717
r_{ks}	0.001	$\Delta\kappa_s$	0.009
θ_{do}	168°		

The Mueller matrix of the sample [eq. (3a)] was then calculated. The calculated Mueller matrix elements $|m_{01}| = 0.306$, $m_{11} = 0.817$, $m_{22} = 0.768$, $m_{23} = 0.039$, and $m_{33} = 0.610$ are marked as vertical lines shown in Fig. 8. They match with the most probable values satisfactorily. With these fitting parameters, we could obtain the quantitative information of the following four independent optical properties: (1) linear-dichroic polarization: $|m_{01}| = 0.3055 > 0$, $\psi = 33.13^o \neq 45^o$; (2) cross-polarized depolarization $\mathcal{D}_v = 0.091$; (3) depolarization $\mathcal{D} = 0.2414 > 0$ and (4) phase retardation $\Delta = 3.25^o$. These best fit parameters and the derived optical depolarization properties of this sample are listed in Table II. These data have shown that this sample exhibits considerable linear dichroism, negligible linear birefringence and large depolarization cause by severe scattering.

TABLE II. BEST FIT MUELLER MATRIX ELEMENTS AND POLARIZATION PROPERTIES

m_{01}	– 0.306	$\mathcal{D}$	0.241
m_{11}	0.817	$\mathcal{D}_v$	0.091
m_{22}	0.768	$\mathcal{D}_u$	0.150
m_{23}	0.039	ψ	33.13°
m_{33}	0.610	Δ	3.25°

E. Tumor and Non-Tumor Tissues Discrimination

To explore the medical clinic applicability, a rat liver biopsy including tumor and non-tumor parts was used to examine their different optical properties and structures. The thickness of each section is about 3 μm.

The distributions $f(|m_{01}|)$ and $f(m_{11})$ are obtained from the corresponding measured images of $|m_{01}|$ and m_{11} and are shown in Figure 10a and 10b. Figure 10a shows that the tumor sample has larger linear dichroism than the non-tumor sample. Since photon scattering reduces the values of m_{11}, Fig. 10b indicates that the tumor sample has smaller photon scattering. These results are consistent with the PSOCT experiment result [19]. The results show that the Mueller Stokes imaging technology is feasible for tissue characterization of medical clinical application.

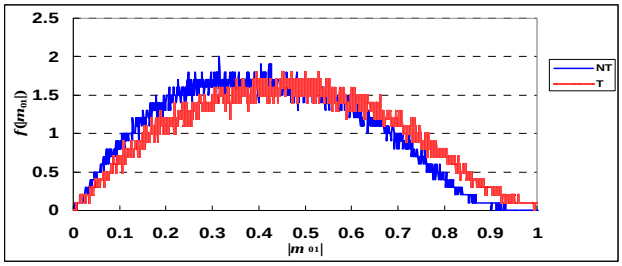

Fig. 10a Measured distribution $f(|m_{01}|)$ for rat liver tissue samples with non-tumor (NT) and tumor (T).

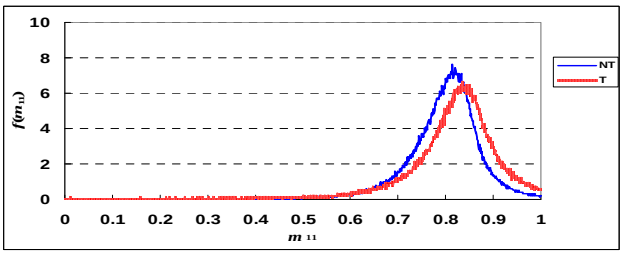

Fig. 10b Measured distribution $f(m_{11})$ for rat liver tissue samples with non-tumor (NT) and tumor (T).

IV. DISCUSSION AND CONCLUSIONS

Using the developed Mueller Stokes imaging technology, the degrees of linear-dichroic polarization and depolarization of a tissue sample can be characterized quantitatively. Particular portions of the sample can also be characterized and compared from the measured imaging data. Using refection optics, this Mueller Stokes imaging technology can be equally used for a thick or non-transmissive sample [10].

In Eq. (4a), $\mathcal{D}_v$ is the cross-polarized depolarization for scattering by a bio-medium [10]. $\mathcal{D}_v = 0$ [or $m_{11} = 1$] for non-scattering samples. The measured m_{11} data in Figures 5 and 8 have clearly provided the quantitative information of photon-scattering in bio-media and others. To our knowledge, the $f(m_{11})$ curve in Figure 8 is the *first* experimental data (with theoretical justification) showing that the photon transport in bio-medium is not perfectly diffusive. Our theory and experiment [12, 20] have provided a foundation for investigating the non-diffusive photon-transport in bio-medium [25, 26].

Polarization-sensitive optical coherence tomography (PSOCT) image has been applied to the discrimination application of bio-tissues [19]. It is similar to our Δ-image. It discriminates only one physical quantity: the phase difference between the s- and p-polarization. A highly coherent laser source is usually required. In this paper, we have demonstrated that the Mueller Stokes imaging technology could provide the tissue signatures of more independent physical quantities. The measured Mueller matrix elements (m_{01}, m_{11}, m_{22}, m_{23} and m_{33}), or the 4 independent optical signatures: m_{01}, m_{11}, $\mathcal{D}$ and Δ of a bio-tissue can be useful as clinical diagnostic tool for medical application. Any light source, either coherent or incoherent, can be used for the measurement. A laser light source is not the only choice.

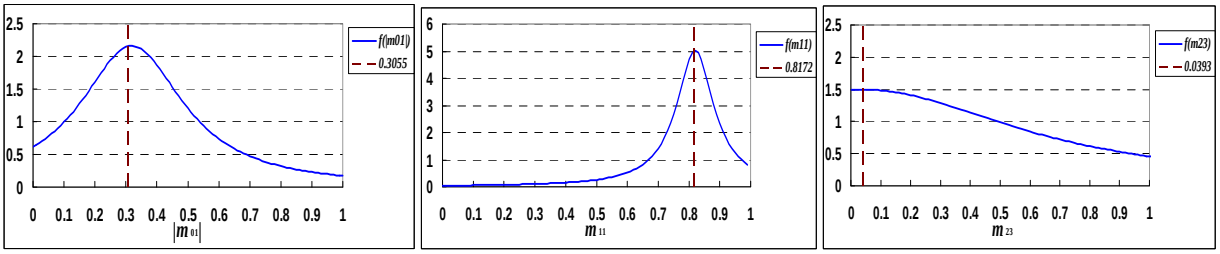

Figure 11 The calculated imaging $f(|m_{01}|)$, $f(m_{11})$ and $f(m_{23})$ with Lorentzian broadenings parameters Δm_{ij} = 0.2, 0.08 and 0.64 respectively.

The transmission Mueller matrix form in Eqs. (2) and (3) is based upon the assumption that the sample surface is also the principal plane. The normal direction (z-axis) is assumed to be a principal axis of the sample. Then the Mueller matrix has the simple form as Eq. (3a) [7]. It is an approximation for mathematical simplicity. Therefore, there exist numerical errors in deriving the five m_{ij}'s [eqs (6a) - (7b)]. These errors could be a possible source of the large broadening of m_{ij} spectra in Figure 8. By assuming Lorentzian line-broadening parameter Δm_{ij} = 0.2, 0.08, 0.64 for m_{01}, m_{11}, m_{23} respectively, the probability distribution functions $f(|m_{01}|)$, $f(m_{11})$ and $f(m_{23})$ for the non-tumor (NT) rat liver tissue are calculated and shown in Fig. 11. They are quite close to the measured data shown in Figure 8. By correlating experiments with the theory, the physical properties of linear dichroism, scattering, depolarization and phase retardation can be determined quantitatively. This

technology is applicable for characterizing the optical properties of the bio-medical samples, both quantitatively and qualitatively.

Tissues have long been treated as optically diffusive media in bio-medical applications. The scattering contribution was usually treated as diffusion theoretically [26 - 28]. The diffusion equation of isotropic photon-density wave (PDW) was widely applied to interpret the data of reflectance spectroscopy [29] and biomedical imaging experiments [30]. However, our measured m_{11} data shown in Figure 8 has clearly demonstrated that the optical property is *not* perfectly diffusive ($m_{11} \neq 0$). Therefore, the polarization/depolarization of non-diffusive anisotropic photon scattering in bio-medical tissue is an interesting topic academically. A complete theory is needed for investigating this issue quantitatively.

The scattering coefficient μ_s of 10% Liposyn II Intravenous emulsion solution were investigated for 400 – 1100 nm based upon the existing diffusion theory [31]. The correlation of μ_s and our measured m_{11} in Fig. 3 is interesting for further investigation.

The major conclusions are listed as follows: (1) The Mueller Stokes imaging technology for a bio-tissue sample is reported. (2) Our experimental data and theoretic fitting results have quantitatively shown that the tissue sample is anisotropic and optically non-diffusive highly scattering medium. (3) The result of 4-signature optical discriminator technology is reported. (4) This multi-signatures technology is an effective and economical clinic diagnostic tool for medical application.

ACKNOWLEDGMENT

This research was partly supported by (1) the NYMU Development of Top-Level International University Program, Ministry of Education, Taiwan, and (2) Research program NSC 98-2112-M-010-004, National Science Council, Taiwan. We thank Professor Fu-Jen Kao for the discussion of the polarimetric microscope technology.

REFERENCES

[1] Z. Chen, H. Ren, Z. Ding, Y. Zhao, J. Miao and J. S. Nelson, “Biomedical imaging: Simultaneous imaging of in situ tissue structure, blood-flow velocity, standard deviation, birefringence and Stokes vectors in human skin,” Optics & Photonics News, 13 (12), Page 14 (2002).

[2] V. V. Tuchin, *Tissue Optics*, *Lightscattering Methods and Instruments for Medical Diagnois* (SPIE Press, 2007).

[3] C. L. Berger, J. S. Craik, D. R. Trentham, J. E. T. Corrie and Y. E. Goldman, “Fluorescence polarization of skeletal muscle fibers labeled with rhodamine isomers on the myosin heavy chain,” Biophys. J. **71**, 3330-3343 (1966).

[4] P. Wu, M. Brasseur, U. Schindler, “Measurement of Specific protease activity utilizing fluorescence polarization,” Anal. Biochem., 247, 83-88 (1997).

[5] G. S. Harms, M. Sonnleitner, G. S. Schutz, H. J. Gruber and T. Schmidt, “Single-molecule anisotropy imaging,” Biophys. J., 77, 2864-2870 (1999).

[6] G. S. Harms, L. Cognet, P.H. M. Lommerse, G. A. Blab, H. Kahr, R. Gamsjager, H. P. Spanink, N. M. Soldatov, C. Romanin and T. Schmidt, “Single-molecule imaging of L-Type Ca^{2+} Channels in Live Cells,” Biophys. J., 81, 2639-2646 (2001).

[7] S.-M. F. Nee, "Polarization measurement," in *The Measurement, Instrumentation and Sensors Handbook*, J. G. Webster, Ed (CRC Press and IEEE Press, 1999), pp. 60.1 - 60.24.

[8] T.-W. Nee and S.-Mie F. Nee, “Infrared polarization signatures for targets”, Proc. SPIE 2469, 231-241 (1995).

[9] T.-W. Nee, S.-M. F. Nee, M. Kleinschmit and S. Shahriar, “Polarization of holographic grating diffraction II. Experiment”, J. Opt. Soc. Am. A **21**, 532-539 (2004).

[10] S.-M. F. Nee and T.-W. Nee, “Principal Mueller matrix of reflection and scattering measured for a one-dimensional rough surfaces”, Opt. Eng. **41**, 994-1001 (2002).

[11] T.-W. Nee, S.-M. F. Nee, D.-M. Yang, and Y.-S. Huang, "Scattering polarization by anisotropic biomolecules," J. Opt. Soc. Am. A 25, 1030-1038 (2008).

[12] T.-W. Nee, S.-M. F. Nee, D.-M. Yang and A. Chiou, "Optical scattering depolarization in a bio-medium with anisotropic bio-molecules",", J. Opt. Soc. Am. A, 26, 1101-1108 (2009).

[13] A. H. Hielscher, A. A. Eick, J. R. Mourant, D. Shen, J. P. Freyer and I. J. Bigio, "Diffuse backscattering Mueller matrices of highly scattering media", Opt. Exp., **1**, 441-453 (1997).

[14] S. Jiao and L. V. Wang, “Two-dimensional depth-depth-resolved Mueller matrix of biological tissue measured with double-beam polarization-sensitive optical coherence tomography”, Optics Letters, **27**, 101-103 (2002).

[15] J. S. Baba, J-R. Chung, A. H. DeLaughter, B. D. Cameron, G. L. Cote, , “Development and calibration of an automated Mueller matrix polarization imaging system”, J. Biomed. Opt. **7**, 341-349 (2002).

[16] X. Liu, S. C. Tseng and M. S. Shahriar, “Complete two-dimensional Mueller metric imaging of biological tissue using heterodyned optical coherence termography”, Frontiers. Opt., FThV3 (2009).

[17] C. E. Saxer, J. F. de Boer, B. H. Park, Y. Zhao, Z. Chen and J. S. Nelson, “High-speed fiber-based polarization-sensitive optical coherence tomography of in vivo human skin”, Optics Letters, 25, 1355 - 1357 (2000).

[18] B. H. Park, C. E. Saxer, S. M. Srinlvas, J. F. de Boer, “In viv burn depth determination by high-speed fiber-based polarization-sensitive optical coherence tomography”, J. Biomed. Opt. 6, 474-479 (2001).

[19] C. C. Wu, Y. M. Wang, L. S. Lu, C. W. Sun, C. W. Lu, M. T. Tsai, C. C. Yang, "Optical birefringence of the hyperlipidemic rat liver with polarization-sensitive optical coherence tomography", J. Biomed. Opt. **12**, 64022 (2007).

[20] Stewart H. Wu, "Polarimetric signature imaging of anisotropic bio-medical tissues", Master Thesis, National Yang-Ming University, Taiwan, June 2010; Proc. SPIE **7556**, 755603-1-6, (2010).

[21] S. F. Nee and T. W. Nee, "Polarization of dipole scattering by randomly oriented ellipsoids," Proc. SPIE **7792**, 779207-1-11 (2010).

[22] H. Ding, J. Q. Lu, K. M. Jacobs, X. H. Hu, "Determination of refractive indices of porcine skin tissues and intralipid at eight wavelengths between 325 and 1557 nm", J. Opt. Soc. Am, A, **22**, 1151-1157 (2005).

[23] H. Ding, J. Q. Lu, W. A. Wooden, P. J. Kragel, X. H. Hu, "Refractive indices of human skin tissues at eight wavelengths and estimated dispersion relations between 300 and 1600 nm", Phys. Med. Biol. **51**, 1479-1489 (2006).

[24] M. Friebel, M. Meinke, "Determination of the complex refractive index of highly concentrated hemoglobin solutions using transmittance and reflectance measurements", J. Biomed. Opt., **10**, 064019-1-5 (2005).

[25] R. Marchesini, A. Bertoni, S. Andreola and A. E. Sichirollo, "Extinction and absorption coefficients and scattering phase functions of human tissues in vitro", Appl. Opt. **28**, 2318-2324 (1989).

[26] R. A. J. Groenhuis, H. A. Ferwerda and J. J. Ten Bosch, "Scattering and absorption of turbid materials determined from reflection measurements. 1: Theory", Appl. Opt. **22**, 2456-2462 (1983).

[27] B. J. Tromberg, L. O. Svaasand, T. T. Tsai, R. C. Haskell, "Properties of photon density waves in multiple-scattering media", Appl. Opt.. **32**, 607-616 (1993).

[28] A. Ishimaru, "Diffusion of light in turbid material", *Appl. Opt.* **28**, 2210-2215 (1989).

[29] H-W. Wang, M. E. Putt, M. J. Emanuele, D. B. Shin, E. Glatstein, A. G. Yodh, and T. M. Busch, "Treatment-induced changes in tumor oxygenation predict photodynamic therapy outcome", Cancer Res. **64**, 7553-7561 (2004).

[30] A. G. Yodh, B. Chance, "Spectroscopy and imaging with diffusing light", Physics Today, **48**, 34-40 (1995).

[31] H. J. van Staveren, C.n J. M. Moes, Jan van Mmarle, S. A Prahl, and M. J. C. van Gemert, "Light scattering in Intralipid-10% in the wavelength range of 400-1100nm", Appl. Opt. **30**, 4507-4514 (1991).

Stewart H. Wu received a M.S. degree from the Institute of Biophotonics at National Yang-Ming University, Taiwan, 2010. He is currently a development engineer with Fab12 Nano Diffusion Engineering Department, Taiwan Semiconductor Manufacturing Company, Ltd., Hsinchu Science Park, Taiwan. During 7/2011-5/2012, he was a senior engineer at LCD Design Dept. of AU Optronics Corporation, Taiwan. He has four publications in the biophotonics research area.

Soe-Mie F. Nee received a M.S. degree and a Ph.D. degree both in physics from the University of Maryland. She is currently a senior scientist with Neopola Optical Analysis Inc., Richmond, CA, U. S. A. She has been a professor with National Central University, and National Yang-Ming University in Taiwan, R. O. C.. During 1983-2006, she was a research physicist at Naval Air Warfare Center, China Lake, CA. She has also been a research associate at Lunar and Planetary Science Laboratory, University of Arizona, and the Physics Department, Technical University of Munich, Germany. Her major interests are polarization physics, polarization optics, starlight polarization, scattering, rough surface effects, optical metrology and polarization in solids and bio-medical materials. She has extensive R/D publications in these fields. She has written a chapter "Polarization measurement," in *The Measurement, Instrumentation and Sensors Handbook*, J. G. Webster, Ed (CRC Press and IEEE Press, 1999).

De-Ming Yang received a Ph.D. degree in life science from National Defense Medical Center, Taiwan. He is currently an associate research investigator at the Department of Medical Research & Education, Taipei Veterans General Hospital, Taiwan and an associate professor at the Institute of Biophotonics, National Yang-Ming University, Taiwan. His major research interests include (1) functional imaging of organelles on single living cells; (2) development of in-vivo, imaging system, nanoscale measuring and imaging of living cells; (3) functional genomics in cancer metastasis. He has extensive R/D publications in these fields.

Arthur Chiou received a Ph.D degree in applied physics from California Institute of Technology. He is currently a professor of the Institute of Biophotonics and the director of the Biophotonics and Molecular Imaging Research Center at National Yang-Ming University, Taiwan. His recent research interest has been in the field of optical manipulation & sensing, and spectroscopic laser microscopy for biomedical applications. He is a senior member of IEEE, a fellow of OSA, a fellow of SPIE, and a fellow of the Photonics Society of Chinese Americans. He is a recipient of NASA "Recognition of Innovative Technical Achievement" Award, SPIE's 1989 Rudolph Kingslake Medal & Award, and ROCOES' Optical Engineering Award.

Tsu-Wei Nee received a Ph.D. degree in solid state physics from the University of Maryland, 1968. He is currently the CEO and a senior scientist with Neopola Optical Analysis, Inc. Richmond, CA, U. S. A. He was a professor with University of Arizona; and National Taiwan University, National Central University, National Tsing-Hua University, National Yang-Ming University, Taiwan. During 1983-2006, he was a research physicist with Naval Air Warfare Center, China Lake, CA. He visited the Technical University of Munich, Germany in 1981-82 as an Alexander von Humboldt Fellow. His research interests include (1) the material optical properties of semiconductors, metal, superconductors and biomedical tissues; (2) electro-optic discrimination sensor technology for remote sensing and bio-medical applications. "Polarimetric optical property of bio-medical materials" is his recent research effort. He has extensive R/D publications in these fields. He is a member of American Physical Society.